LANGMUIR

Article

Film Formation of High T_g Latex Using Hydroplasticization: Explanations from NMR Relaxometry

Benjamin Voogt,[†] Hendrik P. Huinink,*,[†] Sebastiaan J. F. Erich,[†,‡] Jurgen Scheerder,[§] Paul Venema,[‖] Joseph L. Keddie,[⊥] and Olaf C. G. Adan[†,‡]

[†]Department of Applied Physics, Eindhoven University of Technology, P.O. Box 513, Eindhoven 5600 MB, The Netherlands
[‡]TNO (The Netherlands Organization for Applied Scientific Research), P.O. Box 6235, Eindhoven 5600 HE, The Netherlands
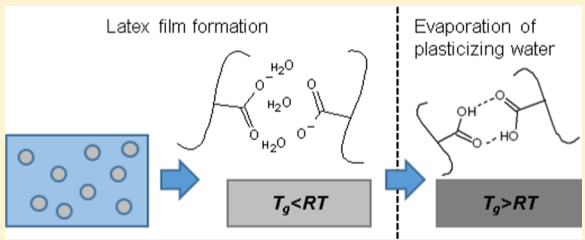[§]DSM Coating resins, P.O. Box 123, Waalwijk 5140 AC, The Netherlands
[‖]Laboratory of Physics and Physical Chemistry of Foods, Wageningen University, P.O. Box 17, Wageningen 6700 AA, The Netherlands
[⊥]Department of Physics, University of Surrey, Guildford GU2 7XH, United Kingdom

(S) *Supporting Information*

ABSTRACT: The film formation of acrylic latex dispersions, containing different amounts of carboxylic acid functional groups by the incorporation of methacrylic acid (MAA), was studied with GARField ^{1}H NMR at various relative humidities (RH). Polymer particles with glass-transition temperatures in the range from 26 to 50 °C formed films at room temperature because of hydroplasticization. It was found that with an increased drying rate due to lower RH, the evaporation flux of water was limited by the latex polymer. Only in the second stage of drying this phenomenon was more obvious with increasing MAA content. ^{1}H NMR relaxometry was used to study the change of hydrogen mobilities during film formation and hardening of the films. This showed that the drying rate itself had no impact on the hydrogen mobility in the latex films as measured via the T_2 relaxation time. Hydrogen mobilities of water and the mobile polymer phase only significantly decrease after most water has evaporated. This implies that the rigidity of the polymers increases with the evaporation of water that otherwise plasticizes the polymer through hydrogen bonding with the carboxylic acid groups. This hardening of the polymer phase is essential for applications in a coating. The hydrogen mobilities were affected by the MAA concentration. Densities of mobile hydrogens increase with increasing MAA content. This is expected if the mobile protons are contained in the MAA groups. The result thus confirms the role of carboxylic acid groups in hydrogen bonding and plasticization of the copolymers. Hydrogen mobilities, however, decrease with increasing MAA content, which is hypothesized to be caused by the formation of dimers of carboxylic acid groups that still hold water. They still enable short-range polymer hydrogen mobility due to hydroplasticization but limit long-range polymer mobility due to interaction between the carboxylic acid groups.

INTRODUCTION

For several decades, latex film formation has been a broadly studied topic. This process is typically divided into three stages.[1,2] One, water evaporates from the aqueous dispersion, resulting in the increased concentration of the polymer particles and overcoming their colloidal stability.[3] Two, particles deform due to capillary effects, forming a close-packed polyhedral structure.[4,5] Three, polymer chains cross the interparticle boundaries through a process called interdiffusion, leading to a cohesive coating.[6,7] It would be more precise to describe film formation as a continuous process rather than a sequential one since these stages overlap in time and different processes may take place simultaneously. For example, it is known that the drying rate of the latex dispersion can lead to heterogeneous distributions of water and polymer in the drying film, with polymer particles accumulating on the latex−air interface.[8,9] This phenomenon can inhibit the evaporation of water from the bulk of the film. When the particles on the surface coalesce, often referred to as skin formation, water evaporation is impeded, resulting in prolonged drying times.[10,11] Pohl and co-workers showed that particle coalescence can overlap with drying and particle deformation.[12]

Only mobile polymers can undergo particle deformation and polymer interdiffusion. Hence, in an application, the user has to deal with the dilemma of choosing between a hard polymer with a volatile plasticizer, which contributes to the emission of volatile organic components (VOCs), or a soft polymer that does not provide good surface protection. This choice between two extremes is called the "film formation dilemma".[2,13,14] However, hydroplasticization, that is, plasticization of polymers by water, offers a way to avoid the problem of VOCs. The

degree of hydroplasticization can be influenced by the polymer chemistry. More specifically, increasing the polymer polarity promotes interaction with water.[15]

The monomer building blocks that are incorporated into the polymer chains interact with water, meaning that they can either bind water, for example, through hydrogen bonding, or repel water due to the hydrophobic nature of the monomers.[15] The effect of polymer composition on the film formation process has been investigated by probing the minimum film formation temperature (MFT) using an MFT bar.[16−18] This technique, however, provides macroscopic information on the drying process without any fundamental basis. Feng and Winnik provided more fundamental proof on the effect of polymer hydrophilicity on polymer interdiffusion.[19] They proved that the water−polymer interaction plays a crucial role in the coalescence of the polymer particles. Incorporation of hydrophilic monomers into the polymer chain appeared to promote polymer interdiffusion.

For acrylic copolymers, examples of highly hydrophilic monomers are acrylic acid and methacrylic acid (MAA).[20,21] These monomers are often used to incorporate charged functionalities via deprotonation of the carboxylic acid groups, enabling colloidal stability of the polymer particles.[22] Moreover, these monomers can bind high amounts of water by hydrogen bonding with the carboxylic acid constituents ensuring hydroplasticization of the copolymers, which lowers their effective glass-transition temperature T_g.[15,23,24] The hydroplasticization effect can be used as a way to obtain film formation of polymers with a dry T_g above the ambient film formation temperature. Hard polymer particles do not deform and coalesce to make a film.[25,26] Hydroplasticized particles are able to form a film, and a hard coating is expected upon the loss of water. However, rigorous investigations of the phenomenon are lacking in the literature.

GARFial ¹H NMR profiling has already been used to study the film formation process of different polymer systems, including alkyd and polyurethane resins and acrylic latex dispersions.[8,11,27−29] Due to its high gradient in the magnetic field, hydrogen distribution profiles can be produced during drying of films, from which drying rates can be derived. Moreover, hydrogen mobilities and densities can be obtained, which can be particularly useful to study how water mobility is affected by the interaction with the polymer, for example, due to hydrogen bonding.

Here, we study the film formation process of acrylic latex dispersions with variable MAA contents using GARFial ¹H NMR to gain valuable insights into the role of the carboxylic acid constituents on water and polymer mobility. The experiments measure the molecular mobility of the polymer phase in the presence of water and as the film hardens after evaporation of water to make a hard coating. Hence, the aim of this study is to understand the influence of the hydroplasticization effect on the film formation behavior of the latex dispersions.

■ EXPERIMENTAL AND THEORETICAL DETAILS

Latex Synthesis. Latex dispersions were synthesized by seeded emulsion polymerization. The monomers methyl methacrylate (MMA; Lucite, >99.8%), MAA (BASF, >99.8%), and butyl acrylate (BA; Arkema, >99.8%) were used as received. The following synthetic procedure is for the latex dispersion containing 2 wt % MAA on total solids. In Table 1, the monomer amounts and the total solid content for each dispersion are listed. The lower limit of MAA was chosen at

Table 1. Monomer Amounts of the Latex Dispersions Used for this Study and the Solid Weight Fractions s_w of the Total Dispersions

monomer fraction (wt % on total solids)			
methacrylic acid	methyl methacrylate	butyl acrylate	s_w (wt %)
2.0	51.0	47.0	33.8
5.0	47.0	48.0	34.1
10.0	40.4	49.6	33.6
15.0	33.7	51.3	30.5
20.0	27.0	53.0	21.7

2% MAA to provide the polymer particles with the necessary colloidal stability. The upper limit was chosen at 20% due to the possibility of gelation of the latex dispersions at a higher MAA content. The ratio of MMA and BA is adjusted for each dispersion to maintain the dry polymer glass-transition temperature at 25 °C according to the Flory−Fox equation.[30] The solid contents are determined gravimetrically. Although the ester moieties of MMA and BA are known to bind water, this will have a negligible influence on the hydroplasticization and concomitant T_g decrease of the copolymers.[15,24]

A 2000 cm³ flask equipped with a thermometer, N₂ inlet, and overhead stirrer was charged with water (799.1 g) and ammonium persulphate (0.35 g). In a funnel, an emulsified monomer feed was prepared by mixing demineralized water (305.97 g), sodium lauryl sulfate (4.62 g of 30 wt % solution in water), methyl methacrylate (MMA, 353.59 g), n-butyl acrylate (n-BA, 325.85 g), and methacrylic acid (MAA, 13.87 g). In another funnel, an initiator solution was charged by dissolving ammonium persulfate (3.12 g) in demineralized water (111.38 g). The reactor was heated to 83 °C, and 5 wt % of the emulsified monomer feed was added to the reactor, and the reaction temperature was allowed to increase to 85 °C. At 83−87 °C, the remainder of the monomer mixture was fed to the reactor in 100 min. At the end of the monomer feed, demineralized water (28.3 g) was used to rinse the funnel holding the monomer mixture. The reaction was kept at 85 °C for 30 min. Next, the batch was cooled to room temperature, and 1,2-benzisothiazolin-3-one (Proxel Ultra 10, 6.9 g of a 10 wt % solution) was added to prevent bacterial and fungal growth in the dispersions, followed by demineralized water (45.3 g). Finally, the batch was filtered through a filter cloth to remove any coagulum formed during the reaction.

Wang and co-workers found that the water loss rate of latex containing a poly(acrylic acid) copolymer was slower in the later stages of drying, when the pH was less than 7.[31] In the present experiments, the pH of the latex dispersions was adjusted by addition of a dilute solution of ammonia (5 wt % in water) under mild stirring. See Table 2 for the pH values obtained. pK_a values for PMAA are

Table 2. Physical Characteristics of the Latices[a]

composition (wt % MAA)	Z_{av} (nm)	Đ	ζ (mV)	pH	η (mPa s)
2	345	0.04	−72	8.1	6
5	323	0.06	−66	7.9	9
10	308	0.05	−51	7.3	17
15	301	0.07	−57	7.1	193
20	293	0.03	−59	7.0	368

[a]Z_{av} is the average particle diameter, Đ is the polydispersity index of the particle size distribution, ζ is the ζ-potential determined at similar pH as the latex dispersion, and η is the latex dispersion viscosity.

reported to be as high as 9.5,[15] which indicates that the latex dispersions studied here might not be fully deprotonated. The pH of the various latex dispersions are set at similar values. Therefore, pH effects are the same in all experiments and not of interest here.

The average particle diameter (Z_{av}), polydispersity (Đ), and ζ-potential at similar pH were determined with a Malvern Zetasizer Nano ZS at 25 °C. Values of ζ indicated good stability of the latex

dispersions. The dispersion viscosities were determined with a viscometer (Brookfield DV-E) with spindle 1 at a speed of 60 rpm. Results of the analyses are listed in Table 2.

Modulated differential scanning calorimetry (TA Instruments Q2000 DSC) analyses were performed on dried material from the latex dispersions to determine the dry polymer T_g values. Results of these measurements are listed Table 3. The DSC thermograms are presented in Figure S1 in the Supporting Information.

Table 3. Results of the Dry Polymer T_g Analyses of the Various Latex Dispersions

composition (wt % MAA)	T_g (°C)	$T_{g,onset}$ (°C)	$T_{g,end}$ (°C)	$T_{g,width}$ (°C)
2	25.9	19.2	32.6	13.4
5	30.2	23.0	37.4	14.4
10	37.3	28.4	46.2	17.8
15	46.9	36.0	57.8	21.8
20	50.2	36.8	63.7	26.9

The T_g values in Table 3 appear to be higher than predicted. An explanation for this is the dimerization of carboxylic acid groups in the dry material, which effectively increases the polymer T_g.[24] This behavior is not predicted by the T_g determination based on the Flory–Fox equation.

Another observation is the increasing width of the T_g transition region $T_{g,width}$ with increasing MAA content. A plausible explanation for this phenomenon is the nonuniformity of the latex particles. Moreover, with increasing MAA content, increasing concentrations of MAA oligomers are expected in the water phase. Due to the low concentration of these oligomers, no distinguishable signal is observed in the GARField ^{1}H NMR experiments.

Wet T_g values were determined using modulated DSC (TA Instruments Q2000 DSC). Samples were sedimented overnight in a centrifuge. Afterward, the serum was decanted, and the residue was used for measurement. Details and results of the measurements are listed in Table 4. The DSC thermograms are presented in Figure S2 in the Supporting Information.

Table 4. Results of the Wet Polymer T_g Analyses of the Various Latex Dispersions[a]

composition (wt % MAA)	T_g (°C)	$T_{g,onset}$ (°C)	$T_{g,end}$ (°C)	$T_{g,width}$ (°C)
2	18.4	≤14.6	22.3	–
5	18.6	≤14.5	22.6	–
10	19.1	≤15.0	23.2	–
15	19.3	≤16.6	22.1	–
20	nm	nm	nm	nm

[a]nm: not measured.

Clearly, T_g values of the wet polymer phase are lower than those of the dry polymer, which is a result of the hydroplasticization effect. Values of $T_{g,width}$ could not be calculated since $T_{g,onset}$ could not be accurately determined. Values of $T_{g,onset}$ are expected to be close to the lower temperature limit (5 °C) of the DSC analyses.

Garfield ^{1}H NMR. The use of GARField ^{1}H NMR imaging and its design and principles have first been described by Glover et al.[32] This technique is a useful tool to study the drying process of thin films. The current equipment has a magnetic field strength of 1.5 T with a static gradient of 42.2 ± 0.2 T/m. An Ostroff–Waugh[33] pulse sequence $(90°_x\text{-}\tau\text{-}[90°_y\text{-}\tau\text{-echo-}\tau]_n)$ is used to obtain signal decays from which T_2 relaxation times of both water and the polymer are obtained. Unless stated otherwise, the echo time $t_e = 2\tau$ used for this study is 40 μs with an acquisition time t_{ac} of 35 μs, resulting in a spatial resolution of 14 μm. The long delay l_d was set at 1.7 s and the number of echoes n at 128. To reduce the signal-to-noise ratio, signal decays were obtained by averaging multiple measurements as follows: for $t < 0.6$ h,

32 averages, for $0.6 < t < 3$ h, 256 averages, and for $t > 3$ h, 1024 averages. The results were normalized with a signal decay of an aqueous 0.025 M CuSO$_4$ solution, with $t_e = 40$ μs, $t_{ac} = 35$ μs, $l_d = 0.3$ s, and $n = 2048$ and 4096 averages.

The NMR setup is equipped with a temperature- and humidity-controlled chamber in which the sample is placed directly onto the RF coil. This sample holder is a 140 μm-thick cover glass, covered with a microscope glass slide having a circular hole with a 10 mm diameter. Herein, 50 μL of latex was placed using a 100 μL volumetric pipette, resulting in a wet coating of about 400 μm thickness. Initially, the sample holder is closed with a silicone stopper to perform a measurement without any initial drying. Subsequently, the cover is removed and sequential drying measurements are performed.

The RH in the climate chamber was set at 46 ± 1, 62 ± 1, or 79 ± 1%. The temperature was set at 23 °C, which is below the T_g of the dry copolymers listed in Table 3.

Ostroff–Waugh signal decays of a latex dispersion at a certain position in the film can be fitted with an exponential decay function

$$S_n(x) = P_n(x) \sum_{k=1}^{N} A_k(x) \exp\left(\frac{-nt_e}{T_{2,k}(x)}\right) + S_0 \tag{1}$$

where $S_n(x)$ is the total signal at time $t = nt_e$ (s), $T_{2,k}(x)$ (s) is the transversal relaxation time of the kth hydrogen pool of the sample with amplitude $A_k(x)$, and S_0 is the signal noise level. $P_n(x)$ is a weighing factor necessary to correct for heterogeneities in the coil profile and echo modulations introduced by the Ostroff–Waugh sequence. $P_n(x)$ is obtained using an aqueous 0.025 M CuSO$_4$ solution. For details, we refer to.[28] With this, eq 1 can be rewritten as

$$I_n(x) = \sum_{k=1}^{N} \frac{A_k(x)}{A_{ref}(x)} \exp\left(\frac{-nt_e}{T_{2,k}(x)}\right) = \sum_{k=1}^{N} \rho_k(x) \exp\left(\frac{-nt_e}{T_{2,k}(x)}\right) \tag{2}$$

where $I_n(x)$ is the relative signal intensity and $\rho_k(x)$ is the relative hydrogen density of the kth hydrogen pool with respect to water. $A_{ref}(x)$ is the signal amplitude obtained with a reference measurement of the 0.025 M CuSO$_4$ solution.

T_2 relaxations can be split into dipole effects $T_{2,dip}$ and a diffusion part $T_{2,diff}$

$$\frac{1}{T_2} = \frac{1}{T_{2,dip}} + \frac{1}{T_{2,diff}} \tag{3}$$

In a previous work, we have shown that with the current experimental conditions with $t_e = 40$ μs, mainly hydrogen relaxations due to dipolar interactions $T_{2,dip}$ are probed.[29] Dephasing due to diffusion in the NMR gradient at this echo time does not play a significant role.

Influence of Relative Humidity on the Drying Rates. The drying rate E (m/s) can be externally limited by the environment or internally limited by transport through the film. In the case of only external limitation, water can evaporate freely from the drying film

$$\frac{dm}{dt} = -AE\rho_w \tag{4}$$

where m is the mass of the evaporated water, t is the evaporation time, A is the area of evaporation, and ρ_w is the density of water. Since E is determined by the water activity difference of the film surface a_f and the environment a, it can be expressed as
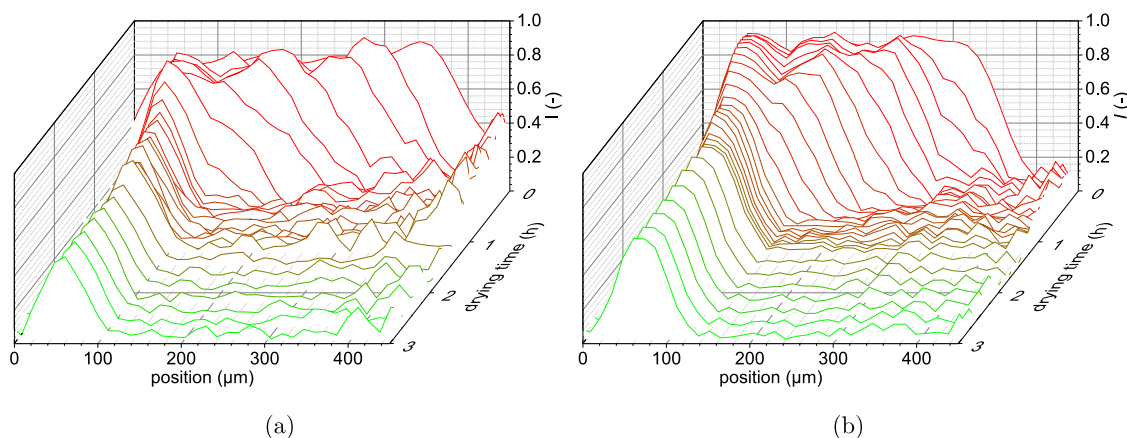
$$E = E'(a_f - a) \tag{5}$$

with E' (m/s) being the weighted drying rate taking account of the water activity difference. With this, eq 4 can be written for E'

$$\frac{dm}{dt'} = AE'\rho_w \tag{6}$$

with the weighted drying time t'

$$t' = (a_f - a)t \tag{7}$$

Figure 1. Hydrogen distribution profiles of a latex containing (a) 2% MAA and (b) 20% MAA drying at 79 ± 1% RH. The color change of the profiles from red to green indicates profiles from early to most recent measurement.

Thus, t' can be calculated if both a and a_f are known. For the latex dispersions, $a_f \approx 1$ and a can be directly calculated from the climate chamber RH

$$RH = a \times 100\% \tag{8}$$

eq 7 can be used to study driving forces for water evaporation from the latex dispersions.

One phenomenon that can limit E is the accumulation of polymer particles at the surface of the latex dispersion layer, forming a barrier for water evaporation. During drying, the distribution of polymer particles in a latex dispersion layer can be affected depending on the evaporation time of water t_{evap} (s)

$$t_{evap} \sim \frac{H}{E} \tag{9}$$

with H (m) being the initial thickness of the latex dispersion layer. The characteristic diffusion time t_{diff} (s) of the polymer particles is inversely proportional to the particle diffusion coefficient D_0 (m^2/s)

$$t_{diff} \sim \frac{H^2}{D_0} \tag{10}$$

with D_0 given by the Stokes–Einstein equation in the dilute regime as

$$D_0 = \frac{kT}{6\pi\eta R} \tag{11}$$

where T (K) is the temperature of the latex dispersion, η (Pa s) is the solvent viscosity, and R (m) is the polymer particle radius. If $t_{diff} \gg t_{evap}$, particles would accumulate on the film–air interface. Basically, the Peclet number described the ratio between advection of particles to the latex film surface due to water evaporation and diffusion of particles from the surface due to Brownian motion. The Peclet number Pe is used to predict this heterogeneous distribution of polymer particles

$$Pe = \frac{t_{diff}}{t_{evap}} = \frac{6\pi\eta HRE}{kT} \tag{12}$$

If $Pe \gg 1$, heterogeneous polymer particle distributions are predicted, whereas for $Pe \ll 1$ homogeneous distributions are expected.

■ RESULTS AND DISCUSSION

Drying Rates of Latex Dispersions. Film formation occurs at 23 °C in the magnetic field, resulting in crack-free and transparent films. This can be understood by the plasticization of the copolymers in the wet latex, lowering the T_g values below the film formation temperature as can be seen in Table 4.[23]

During the drying process of a latex film, bulk water in the film evaporates. Water evaporation rates can be derived from temporal hydrogen distribution profiles obtained with GAR-Field ^{1}H NMR. In Figure 1, examples of hydrogen distribution profiles of the 2 and 20% MAA dispersions during drying at 79 ± 1% RH and 23 °C are shown.

The hydrogen distribution profiles in Figure 1 can be used to determine the film thickness decrease ΔH

$$\Delta H = H(0) - H(t) \tag{13}$$

where $H(0)$ is the film thickness before drying and $H(t)$ is the film thickness at t.

The hydrogen distribution profiles in Figure 1 show spatial signal intensities $I(x)$, proportional to mobile hydrogen densities according to eq 2, during drying of the latex film. This clearly shows latex-air fronts, which are receding faster for the 2% MAA latex dispersion. This front shows a gradient, which is caused by the low spatial resolution of approximately 14 μm and averaging over multiple measurements as described in the Experimental Section. The drying surface is at the receding right side of the profiles, whereas position 0 reflects the bottom of the latex film. ΔH of the latex dispersion layer can be estimated from the front and bottom positions, which are taken at $I = 0.5I_{max}$, with I_{max} being the maximum signal intensity of each profile. In Figure 2a,b ΔH as a function of drying time is shown for the 2 and 20% MAA latex dispersions.

Figure 2 shows two phases. First, a linear increase of ΔH is observed, which is a result of the water evaporation and the concomitant shrinkage of the film. Second, ΔH stabilizes to a constant thickness. In this phase, further evaporation of residual water in the coating does not significantly change ΔH. From linear fits of the plots in the first phase, E can be determined from the slopes.
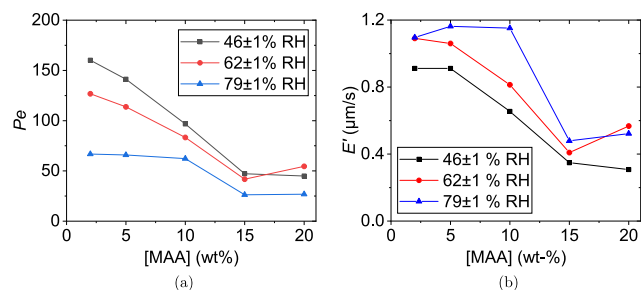
The linear fits for the 2% MAA latex dispersion in Figure 2a clearly show an increased E with decreasing RH, which is in line with the expectation that a higher ambient RH leads to slower evaporation of water. The results for the 20% MAA latex dispersion shown in Figure 2b, however, do not show this relation, since at 46 ± 1% RH E appears to be lower than at the other, higher RH's. This already indicates that additional phenomena are influencing E.

To obtain a better insight into the cause of the deviations in the drying behavior, eq 12 is used to calculate Pe for all of the dispersions at the different RH's. For this, E values obtained from the linear fits as shown in Figure 2a,b were used. Results
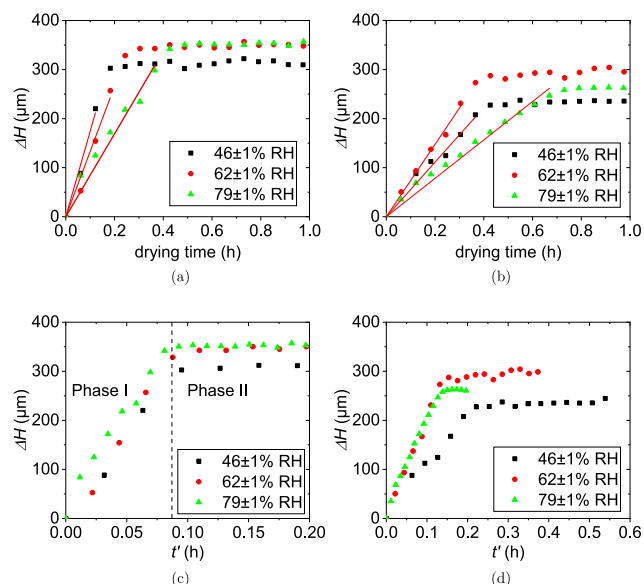
Figure 2. (a) and (b): ΔH of the 2% and 20% MAA latex dispersions, respectively, dried at 79 ± 1, 62 ± 1, and $46 \pm 1\%$ RH. The red lines represent linear fits with slope E. (c) and (d): ΔH of the 2% and 20% MAA latex dispersions, respectively, dried at 79 ± 1, 62 ± 1, and $46 \pm 1\%$ RH, with the drying time t adjusted with the water activity difference $(a_f - a)$ to t'. The dashed line indicates the transition point from shrinking films to films with a stable film thickness.

are shown in Figure 3a. Moreover, eq 7 was used to calculate the weighted drying time t'. Figure 2c and d show ΔH as a

Figure 3. (a) Pe dependence on the latex dispersion MAA content ([MAA]). (b) Dependence of E' on [MAA].

function of t' for the 2 and 20% MAA latex dispersions, respectively. E' is obtained from linear fits of the slopes, which can be used to evaluate how drying rates are affected by the climate chamber RH. The results are shown in Figure 3b.

The values found for E, and therefore E', are significantly higher than those found in the literature for pure water or latex films drying in static air.[11,34,35] It should be noted, however,

that the values reported here are obtained with an airflow in the climate chamber.

As discussed, fast drying of latex dispersions can result in heterogeneous water−polymer distributions due to accumulation of polymer particles on the latex−air interface. Figure 3 clearly shows that $Pe \gg 1$ for all of the latex dispersions at any of the applied RH, indicating that this particle accumulation is indeed taking place. This could inhibit E. Although the hydrogen distribution profiles shown in Figure 1 are expected to show a gradient in the NMR signal, similar to those found by Carter who showed the appearance of a lower signal intensity at the latex film surface,[11] this is not visible due to the low spatial resolution of the current profiles.

E is proportional to the water activity difference $a_f - a$, as is schematically shown in Figure 4, and is expected to be inversely proportional to the polymer barrier thickness δ

$$E \propto \frac{a_f - a}{\delta} \tag{14}$$

According to eq 14, a decrease of a_f or an increase of δ would result in a decrease of E during drying. The data in Figure 2, however, show linear slopes, and Figure 3b shows that E is proportional to $a_f - a$. This implies that a_f remains constant during drying and the increase of δ does not affect the evaporation of water. This implies that evaporation of water is not hindered by particle accumulation due to high Pe values. Hence, no significant particle deformation and coalescence of the accumulated particle take place.
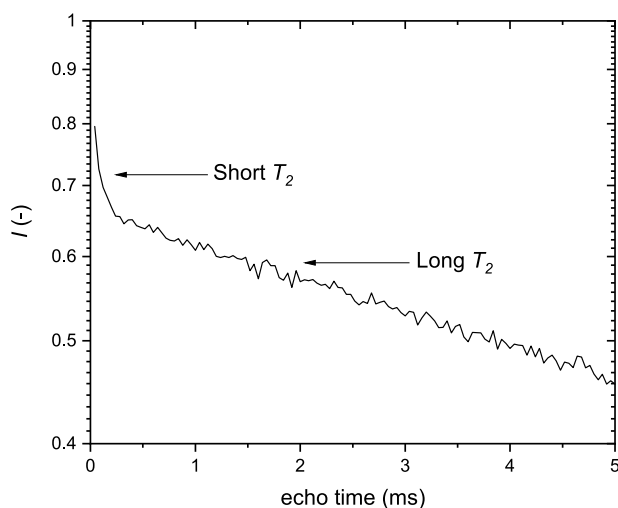
The values of E' in Figure 3b show a trend of decreasing E' with an increasing MAA concentration [MAA]. This suggests that the increased MAA content of the particles plays a role in the drying behavior of the latex dispersions. A plausible explanation would be that hydrogen bonding of carboxylic acid groups with water can inhibit E.[36] Therefore, the effect of MAA will be considered next.

Hydrogen Mobilities during Film Formation. *Analysis of the Ostroff−Waugh Signal Decay.* As was shown in the previous section, the values of E and E' can be affected by the presence of MAA and thus carboxylic acid constituents of the polymers. Figure 3b shows that increasing the MAA concentration in the polymer results in a decrease of E'. To determine the influence of MAA on the drying process and film formation of latex polymers with T_g below the ambient temperature, ^{1}H NMR relaxometry has been used to study the water and polymer hydrogen mobilities during drying. As an example, in Figure 5, an Ostroff−Waugh decay of the 2% MAA latex dispersion before drying is shown.

From the Ostroff−Waugh decays, T_2 relaxation times can be obtained. These relaxation times are a measure of hydrogen mobility and hence water and polymer mobility. Increasing values indicate higher mobilities. For each observed T_2, a
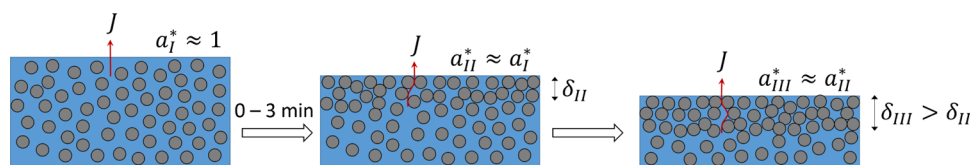
Figure 4. Schematic drawing of a drying latex film resulting in heterogeneous water and polymer distributions. The water activity on the latex surface a_f is approximately 1 and remains constant during drying of the latex films, as reflected by a constant E. The polymer barrier thickness δ, which is formed rapidly between the first two ^{1}H NMR measurements (0−3 min.), is expected to increase during drying since $Pe \gg 1$. The water evaporation flux J is not affected by this, meaning that the surface of the latex layer remains open during the bulk drying of the latex films.

Figure 5. Ostroff−Waugh decay of the 2% MAA latex dispersion before drying.

Figure 6. (a) and (b): Short $T_{2,\text{short}}$ transversal relaxation times and proton densities ρ_{short} of the 2% MAA latex dispersion as a function of drying time. (c) and (d): Long $T_{2,\text{long}}$ transversal relaxation times and proton densities ρ_{long} of the 2% MAA latex dispersion as a function of drying time.

Figure 7. (a) Short hydrogen densities ρ_{short} and (b) long hydrogen densities ρ_{long} of all latex dispersions versus the relative film thickness $H_{\text{min}}/H(t)$ of the coatings during drying at $79 \pm 1\%$ RH. Dashed lines are drawn to guide the eye.

hydrogen density ρ is also obtained, which is a measure of the density of hydrogens at a given mobility.

The Ostroff−Waugh decay in Figure 5 and subsequent decays during drying of the various latex dispersions show the presence of two hydrogen pools with different mobilities. This means that they can be fit with eq 2 using $k = 2$ resulting in a short $T_{2,\text{short}}$ and long $T_{2,\text{long}}$ relaxation with their respective hydrogen densities ρ_{short} and ρ_{long}. $T_{2,\text{short}}$ was previously attributed to hydrogens of rigid polymer domains in the latex, whereas $T_{2,\text{long}}$ is attributed to hydrogens of water and soft polymer domains.[29] These soft polymer domains may arise from an MAA-enriched surface layer of the particles, which is also indicated by the DSC analyses as discussed in the Experimental Section.

Effect of RH on Hydrogen Mobilities. The transversal relaxation times T_2 and the hydrogen densities ρ during the film formation process of each latex dispersion at the various RH values can provide valuable insights into the influence of latex MAA content on the process. Figure 6 shows T_2 and ρ as a function of drying time t for the 2% MAA latex dispersion.

The short relaxation time $T_{2,\text{short}}$ in Figure 6a does not show any significant variation during drying. This could indicate the presence of a rigid polymer fraction with low hydrogen mobility, having no apparent interaction with water. The hydrogen density ρ_{short} shown in Figure 6b, however, increases during the drying process.

Since ρ_{short} represents the hydrogen density of a rigid polymer phase, its value would scale with the polymer concentration during drying. Relative polymer concentrations can be obtained from the minimum film thickness H_{min}, where the solid weight s_w approaches 100%, and the thickness of the latex film at any point during the drying process $H(t)$. In Figure 7a, ρ_{short} is shown versus $H_{\text{min}}/H(t)$ of films of the various latex dispersions dried at $79 \pm 1\%$ RH. This indeed shows linear behavior of ρ_{short} with the latex solid content for all dispersions and that ρ_{short} increases due to concentrating of the polymer phase.

The long relaxation time $T_{2,\text{long}}$ in Figure 6c shows a gradual decrease down to a constant value. This behavior was explained before by the evaporation of water and the decrease in polymer hydrogen mobility.[29] The relative hydrogen density ρ_{long} for $T_{2,\text{long}}$ decreases, as can be seen in Figure 6d. Figure 7b
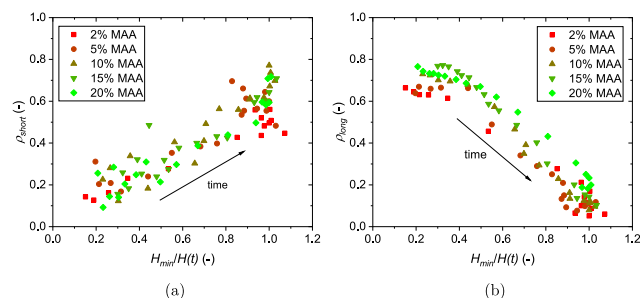
shows the correlation of ρ_{long} with $H_{\text{min}}/H(t)$, proving the relation between the decrease of ρ_{long} and the loss of mobile hydrogen atoms due to evaporation of water. Although Figure 7 clearly shows the concentration effect, a more in-depth analysis of $T_{2,\text{long}}$ is needed to elucidate the role of water−polymer interaction on hydrogen mobility.

To investigate the influence of the RH in the climate chamber on the bulk drying process of the latex dispersion films, the relation between $T_{2,\text{long}}$ and the corresponding ρ_{long} can be investigated for each dispersion. In Figure 8a, $T_{2,\text{long}}$ is shown as a function of ρ_{long} for the 2% MAA dispersion at the various RH values. Evidently, E controlled via the RH has no impact on the relaxation behavior of the hydrogens, which supports the results in Figure 3b that the RH does not significantly influence the drying process of the latex dispersions.

The MAA content strongly influences the hydrogen relaxation behavior. Figure 8b shows $T_{2,\text{long}}$ as a function of ρ_{long} for all dispersions dried at $79 \pm 1\%$ RH. When comparing the hydrogen mobilities during drying of the different latex dispersions, clear differences are found. Hydrogen mobilities decrease with increasing MAA content of the latex at a given
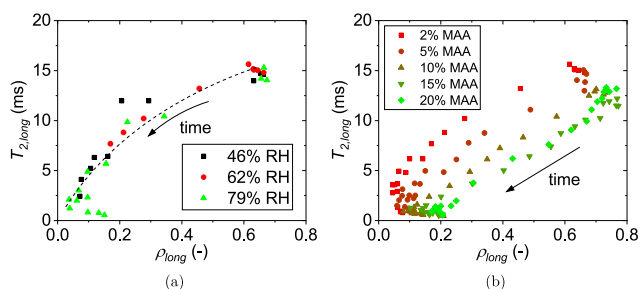
Figure 8. (a): $T_{2,\text{long}}$ as a function of ρ_{long} at the various RH values for the 2% MAA latex dispersion. (b): $T_{2,\text{long}}$ as a function of ρ_{long} for the various latex dispersions at 79 ± 1% RH.

ρ_{long}. The decrease of water hydrogen mobility due to hydrogen bonding with carboxylic acid groups can explain this behavior.

Influence of MAA Content on Film Formation. As was shown in Figure 6, both ρ_{long} and $T_{2,\text{long}}$ decrease and ρ_{short} increases during drying of the latex dispersions. A better understanding of the effect of water evaporation on the hydrogen density and mobility changes can be obtained by plotting $T_{2,\text{long}}$ and the hydrogen densities ρ_{short} and ρ_{long} as a function of H, shown in Figure 9 for the 10% MAA latex dispersion dried at 79 ± 1% RH.
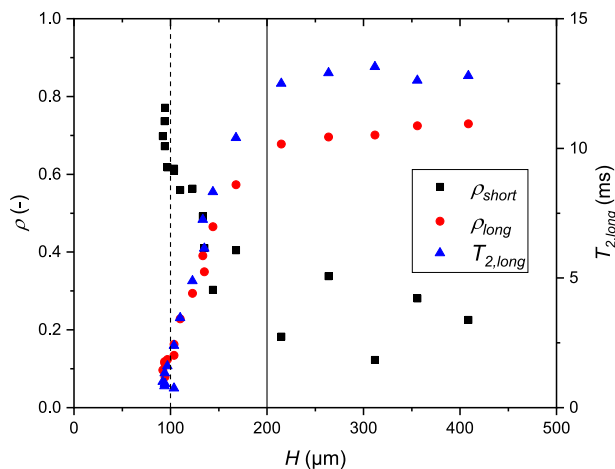
Figure 9. ρ_{short}, ρ_{long}, and $T_{2,\text{long}}$ as a function of the latex coating thickness during drying of the 10% MAA latex dispersion at 79 ± 1% RH. The solid line represents H at which $T_{2,\text{long}}$ gradually decreases, coinciding with the close packing of the latex particles. The dashed line indicates the minimum film thickness H_{min} at which $T_{2,\text{long}}$ shows a sharp decrease.

Clearly, during an initial drying stage, $T_{2,\text{long}}$ does not change significantly. This indicates that the overall hydrogen mobility present in this pool during this stage of the drying process is hardly affected by the evaporation of water. The solid content of the latex dispersion at this point is approximately 68 wt %. Previously, it was found that at this point the drying film reaches its closest particle packing.[29] When H approaches H_{min}, $T_{2,\text{long}}$ shows a sharp decrease, indicating a decrease of hydrogen mobility, when most water has evaporated.

To provide a better insight into the hydrogen mobilities near the end of the drying process, Figure 10 shows the inverse of $T_{2,\text{long}}$ as a function of ρ_{long}. Even after the coatings reached their minimum thickness and the minimum value of ρ_{long}, the hydrogen mobilities still decrease drastically. This shows that
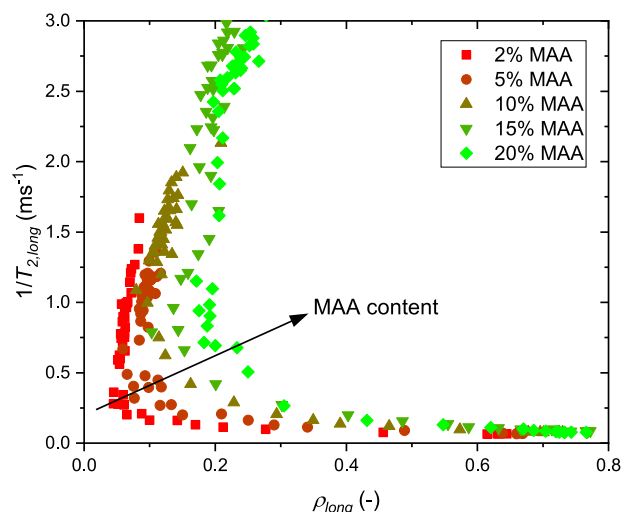
Figure 10. Inverse of $T_{2,\text{long}}$ as a function of ρ_{long}. The arrow is drawn to stress the effect of increasing MAA content on the hydrogen mobility of the various latex dispersions during the drying process.

the rigidity of the polymers still increases, most likely due to continued evaporation of small amounts of water that provide a high degree of hydroplasticization to the polymers. At this point, differences between the various latex dispersions are clearly visible.

Apparently, with an increase in MAA content, the rigidity of the polymers at similar ρ_{long} increases. This can be explained by the dimerization of carboxylic acid constituents on the polymer chains (Figure 11), resulting in a lower polymer mobility with
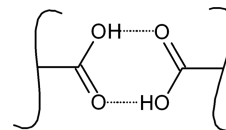

Figure 11. Schematic drawing of a dimer of carboxylic acid constituents on copolymer chains.

increasing MAA content. The density of mobile hydrogens, however, decreases to lower values with decreasing MAA content as indicated by the lower values of ρ_{long} in the dried coatings. This indicates a lower water content of the coating at the end of the drying process due to the lower polarity of the latex coating.

Fourier transform infrared-Attenuated total reflection (FTIR-ATR) measurements support this hypothesis, as dimers of carboxylic acid were shown to be present. For details on measurements and results, we refer to our previous work.[24] For the 15 and 20% MAA films, however, charged carboxylate groups are still present, apparent from a band at 1542 cm^{-1} representing COO^{-} stretch vibrations as shown in Figure 12.[31] This would imply that evaporation or partial evaporation of ammonia during the drying process leads to protonation of the carboxylate groups. Since carboxylic acid groups bind less water (1.3 mol/mol COOH) than carboxylate groups (11.3 mol/mol COO^{-}),[15] the degree of hydroplasticization of the copolymers decreases significantly.

■ DISCUSSION

The study of the drying process of the various latex dispersions at different RH's has shown that variations of the MAA content
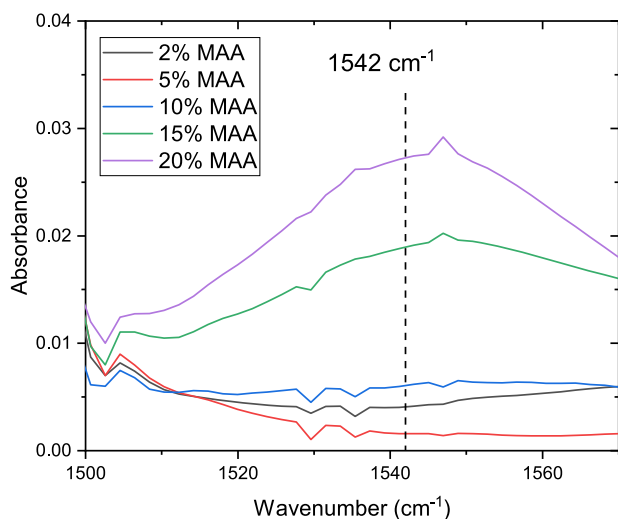
Figure 12. FTIR-ATR absorbance spectra of the dried latex films in the characteristic region for ionic interaction of carboxylate constituents. The spectra were shifted vertically for the sake of clarity.

of the polymer, and therefore the carboxylic acid content, affect the drying behavior of films of the latex dispersions. Figure 13 shows a schematic picture of the observed phenomena, divided into four phases. Accumulation of polymer particles occurs in phase I, followed by bulk water evaporation until close packing of particles in phase II, evaporation of water between packed particles and particle deformation in phase III, and evaporation of plasticizing water resulting in rigidification of the polymer in phase IV.

During phase I of the drying process, particles accumulate on the latex−air interface. It was shown that heterogeneous distributions are expected to occur for all latex dispersions based on the estimation of the Pe values. Particle accumulation occurs early during the drying process, which is followed by a constant evaporation rate E. This implies that an increase of the particle boundary thickness δ at the interface does not slow down water evaporation further. Hence, no particle deformation or interdiffusion occurs, which would result in a

continuous decrease of E. Therefore, the accumulated particle layer allows water to evaporate via a tortuous pathway.

The bulk drying of water in phase II of the drying process studied by ^{1}H NMR relaxometry provides a deeper understanding of the drying process. The two relaxation times found can be ascribed to hydrogens with different mobilities, with $T_{2,short}$ reflecting the mobility of hydrogens of more rigid polymeric parts and $T_{2,long}$ reflecting more mobile hydrogens. In a previous work,[29] it was shown that hydrogens from both water and polymer contribute to $T_{2,long}$ and ρ_{long} and that $T_{2,short}$ and ρ_{short} arise from more rigid polymer domains. From the T_2 relaxation times and the corresponding hydrogen densities of the latex dispersions during drying, three important observations are made. One, hydrogens of the rigid polymer fraction reflected by $T_{2,short}$ and ρ_{short} increase linearly with the solid fractions of the latex dispersions during drying and do not significantly interact with water, as is obvious from the constant values for $T_{2,short}$. Two, for the individual latex dispersions, variations of E set by the climate chamber RH do not affect the hydrogen relaxations in the more mobile hydrogen phase represented by $T_{2,long}$ and ρ_{long}. Thus, only E is affected. This indicates that E does not affect water−polymer interaction or polymer interdiffusion. Three, between the individual latex dispersions, differences in hydrogen mobilities are observed from the $T_{2,long}$ data. At similar hydrogen densities ρ_{long}, mobilities appear to decrease with increasing carboxylic acid content. An explanation for this behavior is the interaction of water with carboxylic acid groups through hydrogen bonding, which decreases overall hydrogen mobilities.

Upon evaporation of water, two different processes take place that affect $T_{2,long}$ and ρ_{long}: a decrease of hydrogen atoms due to the evaporation of water and a decrease of hydrogen mobility in this phase due to increased rigidity of polymer segments, which were previously plasticized by water. Initially, as depicted by phase II in Figure 13, the evaporation of bulk water does not appear to impact $T_{2,long}$ significantly, indicating that the hydrogen density and mobility of the mobile phase are hardly affected by the loss of water. Only when close packing of the particles is reached, $T_{2,long}$ starts decreasing due to confinement of water. Only when the bulk water has
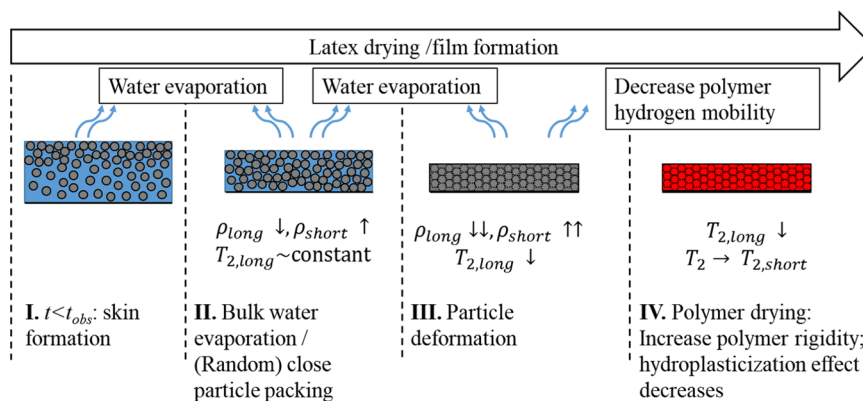
Figure 13. Schematic illustration of the four phases during the drying process of the various latex dispersions. Different phenomena can be distinguished. I. Particle accumulation on the latex surface occurs early during the drying process. II. Water evaporation continues, with increasing ρ_{short} and decreasing ρ_{long}. $T_{2,long}$ remains constant. III. After close packing of the particles, ρ_{short} increases faster and ρ_{long} decreases faster. $T_{2,long}$ also starts decreasing gradually. IV. When the film thickness reaches the minimum film thickness, hydroplasticization of the polymer chains disappears due to the low amount of water present in the coatings, resulting in a decreased polymer hydrogen mobility. Due to this, $T_{2,long}$ shows a sharp decrease.

evaporated and the thickness of the film reaches the minimum film thickness by closest packing of the particles, represented by phase IV in Figure 13, $T_{2,long}$ sharply decreases. Apparently, the rigidity of the polymer increases due to a decreased hydroplasticization of polymer segments. At this point, clear differences appear between the various latex dispersions. ρ_{long} decreases to lower values with decreasing MAA content. This is logical since carboxylic acid groups can bind high amounts of water (1.3 mol/mol −COOH and 11.3 mol/mol −COO⁻) and as such account for a high degree of hydroplasticization.[15]

The relaxometry data in Figure 10 show that the mobility of the polymer hydrogens in the mobile phase decreases with increasing MAA content. For these latex dispersions, it was found that carboxylic acid groups form dimers, which can hold water.[24] Hence, this may be due to the formation of these "open" dimers of carboxylic acid groups. Polymer hydrogen mobility is still limited, however, due to this dimerization.[37,38]

CONCLUSIONS

Acrylic copolymers with glass-transition temperature T_g values above 23 °C were film-formed at that temperature because of hydroplasticization resulting from the presence of MAA monomers. This hydroplasticization during film formation and film hardening of acrylic latex dispersions with different concentrations of methacrylic acid (MAA), ranging from 2 to 20 wt % on total solid content of the dispersions, was studied at various RH values by NMR techniques.

It is found that the polymer MAA content affects the film formation process of the latex dispersions. The drying rate E decreases with increasing MAA content. In a later stage of the drying process, when the latex film thickness approaches its minimum thickness, rigidity of the polymers increases. Due to evaporation of residual water that enabled hydroplasticization of the polymers, polymer segments become less mobile.

It is shown that varying the RH of the climate chamber, and hence the drying rate, does not affect the water−polymer interaction of the various latex dispersions during drying. Hydrogen mobilities at similar hydrogen densities, however, appear to decrease with increasing carboxylic acid content. This phenomenon is explained by the hydrogen-bonding interaction between water and carboxylic acid groups, resulting in an overall decrease of hydrogen mobility in the dispersion.

This work shows that polymers with hydrophilic functional groups can be used to form films at room temperature from polymers that are glassy when dry. Because the hydroplasticized polymer phase hardens as the water evaporates and water is not a volatile organic component (VOC), this material offers a way to solve the film formation dilemma. Although the typical MAA content of a latex for paints is between 2 and 5 wt % on total solids,[20] the results are a viable starting point for further development of fully hydroplasticizable binders.

ASSOCIATED CONTENT

ⓈSupporting Information

The Supporting Information is available free of charge on the ACS Publications website at DOI: 10.1021/acs.langmuir.9b01353.

DSC thermograms of the wet and dry T_g analyses of the various latex dispersions (PDF)

AUTHOR INFORMATION

Corresponding Author
*E-mail: h.p.huinink@tue.nl. Phone: +31 (0)40 2475375.
ORCID
Benjamin Voogt: 0000-0001-6483-9452
Joseph L. Keddie: 0000-0001-9123-183X
Notes
The authors declare no competing financial interest.

ACKNOWLEDGMENTS

REFERENCES

(1) Vanderhoff, J. W.; Bradford, E. B.; Carrington, W. K. Transport of Water through Latex Films. In *Journal of Polymer Science Part C: Polymer Symposium*; Wiley Subscription Services, Inc., A Wiley Company: NY, 1973; pp 155−174.

(2) Keddie, J. L.; Routh, A. F. *Fundamentals of Latex Film Formation*, 1st ed.; Pasch, H., Ed.; Springer: Dordrecht, The Netherlands, 2010.

(3) Visschers, M.; Laven, J.; van der Linde, R. Forces operative during film formation from latex dispersions. *Prog. Org. Coat.* **1997**, *31*, 311−323.

(4) Brown, G. L. Formation of films from polymer dispersions. *J. Polym. Sci. A.* **1956**, *22*, 423−434.

(5) Visschers, M.; Laven, J.; German, A. L. Current understanding of the deformation of latex particles during film formation. *Prog. Org. Coat.* **1997**, 39−49.

(6) Russell, T.; Deline, V.; Dozier, W.; Felcher, G.; Agrawal, G.; Wool, R.; Mays, J. Direct observation of reptation at polymer interfaces. *Nature* **1993**, *365*, 235−237.

(7) Wang, Y.; Winnik, M. A. Polymer diffusion across interfaces in latex films. *J. Phys. Chem. A.* **1993**, *97*, 2507−2515.

(8) Gorce, J.-P.; Bovey, D.; McDonald, P. J.; Palasz, P.; Taylor, D.; Keddie, J. L. Vertical water distribution during the drying of polymer films cast from aqueous emulsions. *Eur. Phys. J. E* **2002**, *8*, 421−429.

(9) Ma, M.; Jiang, K.; Qiu, G.; Wang, D.; Hu, X.; Jin, X.; Chen, Z. G. Fundamental study on electro-reduction of solid titania in molten calcium chloride. *J. Rare Earths* **2005**, *23*, 46−49.

(10) Mallégol, J.; Bennett, G.; Mcdonald, P. J.; Dupont, O.; Keddie, J. L. Skin Development During the Film Formation of Waterborne Acrylic Pressure-Sensitive Adhesives Containing Tackifying Resin. *J. Adhes.* **2006**, *82*, 217−238.

(11) Carter, F. T.; Kowalczyk, R. M.; Millichamp, I.; Chainey, M.; Keddie, J. L. Correlating particle deformation with water concentration profiles during latex film formation: Reasons that softer latex films take longer to dry. *Langmuir* **2014**, *30*, 9672−9681.

(12) Pohl, K.; Adams, J.; Johannsmann, D. Correlation between particle deformation kinetics and polymer interdiffusion kinetics in drying latex films. *Langmuir* **2013**, *29*, 11317−11321.

(13) Georgiadis, A.; Bryant, P. A.; Murray, M.; Beharrell, P.; Keddie, J. L. Resolving the film-formation dilemma with infrared radiation-assisted sintering. *Langmuir* **2011**, *27*, 2176−2180.

(14) Geurts, J.; Bouman, J.; Overbeek, A. New waterborne acrylic binders for zero VOC paints. *J. Coat. Technol. Res.* **2008**, *5*, 57−63.

(15) Tsavalas, J. G.; Sundberg, D. C. Hydroplasticization of polymers: Model predictions and application to emulsion polymers. *Langmuir* **2010**, *26*, 6960−6966.

(16) Dobler, F.; Pith, T.; Lambla, M.; Holl, Y. Coalescence mechanisms of polymer colloids. *J. Colloid Interface Sci.* **1992**, *152*, 1−11.

(17) Sperry, P. R.; Snyder, B. S.; O'Dowd, M. L.; Lesko, P. M. Role of Water in Particle Deformation and Compaction in Latex Film Formation. *Langmuir* **1994**, *10*, 2619−2628.

(18) Hasanzadeh, I.; Mahdavian, A. R.; Salehi-Mobarakeh, H. Particle size and shell composition as effective parameters on MFFT for acrylic core-shell particles prepared via seeded emulsion polymerization. *Prog. Org. Coat.* **2014**, *77*, 1874−1882.

(19) Feng, J.; Winnik, M. Effect of water on polymer diffusion in latex films. *Macromolecules* **1997**, *9297*, 4324−4331.

(20) Weiss, K. D. Paint and Coatings: A Mature Transition Industry. *Prog. Polym. Sci.* **1997**, *22*, 203−245.

(21) Swift, G. *Encyclopedia of Polymer Science and Technology*, 4th ed.; John Wiley & Sons: 2002; Vol. *1*, pp 79−96.

(22) Tracton, A. A. *Coatings Technology Handbook*, 3rd ed.; CRC Press: Boca Raton, FL, 2006; pp 48−53.

(23) Jiang, B.; Tsavalas, J.; Sundberg, D. Measuring the glass transition of latex-based polymers in the hydroplasticized state via differential scanning calorimetry. *Langmuir* **2010**, *26*, 9408−9415.

(24) Voogt, B.; Huinink, H.; Peeters, L.; Erich, B.; Scheerder, J.; Adan, O. Hydroplasticization of latex films with varying methacrylic acid content. *Polymer* **2019**, *166*, 206−214.

(25) Lee, W. P.; Routh, A. F. Why do drying films crack? *Langmuir* **2004**, *20*, 9885−9888.

(26) Tirumkudulu, M. S.; Russel, W. B. Cracking in drying latex films. *Langmuir* **2005**, *21*, 4938−4948.

(27) Erich, S. J. F.; van der Ven, L. G. J.; Huinink, H. P.; Pel, L.; Kopinga, K. Curing processes in solvent-borne alkyd coatings with different drier combinations. *J. Phys. Chem. B* **2006**, *110*, 8166−8170.

(28) Baukh, V.; Huinink, H. P.; Adan, O. C.; Erich, S. J.; van der Ven, L. G. Water-Polymer Interaction during Water Uptake. *Macromolecules* **2011**, *44*, 4863−4871.

(29) Voogt, B.; Huinink, H.; Erich, B.; Scheerder, J.; Venema, P.; Adan, O. Water mobility during drying of hard and soft type latex: Systematic GARField1H NMR relaxometry studies. *Prog. Org. Coat.* **2018**, *123*, 111−119.

(30) Fox, T. G. Influence of Diluent and of Copolymer Composition on the Glass Temperature of a Polymer System. *Bull. Am. Phys. Soc.* **1956**, *1*, No. 123.

(31) Wang, T.; Canetta, E.; Weerakkody, T. G.; Keddie, J. L.; Rivas, U. pH dependence of the properties of waterborne pressure-sensitive adhesives containing acrylic acid. *ACS Appl. Mater. Interfaces* **2009**, *1*, 631−639.

(32) Glover, P. M.; Aptaker, P. S.; Bowler, J. R.; Ciampi, E.; McDonald, P. J. A novel high-gradient permanent magnet for the profiling of planar films and coatings. *J. Magn. Reson.* **1999**, *139*, 90−97.

(33) Ostroff, E. D.; Waugh, J. S. Multiple spin echos and spin locking in solids. *Phys. Rev. Lett.* **1966**, *16*, 1097−1099.

(34) Tsuji, M.; Nakahara, H.; Moroi, Y.; Shibata, O. Water evaporation rates across hydrophobic acid monolayers at equilibrium spreading pressure. *J. Colloid Interface Sci.* **2008**, *318*, 322−330.

(35) Ekanayake, P.; McDonald, P. J.; Keddie, J. L. An experimental test of the scaling prediction for the spatial distribution of water during the drying of colloidal films. *Eur. Phys. J.: Spec. Top.* **2009**, *166*, 21−27.

(36) Tang, J.; Dimonie, V. L.; Daniels, E. S.; Klein, A.; El-Aasser, M. S. Study of the Drying Behavior of Model Latex Blends during Film Formation: Influence of Carboxyl Groups. *Macromol. Symp.* **2000**, *155*, 139−161.

(37) Dong, J.; Ozaki, Y.; Nakashima, K. Infrared, Raman, and near-infrared spectroscopic evidence for the coexistence of various hydrogen-bond forms in poly(acrylic acid). *Macromolecules* **1997**, *30*, 1111−1117.

(38) Hoerter, M.; Oprea, A.; Bârsan, N.; Weimar, U. Chemical interaction of gaseous ammonia and water vapour with polyacrylic acid layers. *Sens. Actuators, B* **2008**, *134*, 743−749.